AIAA JOURNAL
Vol. 47, No. 9, September 2009

Experimental Investigation of Screech-Tone Characteristics of Jet Interaction with a Flat Plate

Mohammed K. Ibrahim,* Takashi Sawai,† Kimihito Obase,‡ Koichi Mori,§ and Yoshiaki Nakamura¶
Nagoya University, Nagoya 464-8603, Japan

DOI: 10.2514/1.37077

The screech-tone characteristics of an underexpanded jet in the vicinity of a flat plate in which the jet is emitted from a circular sonic nozzle and interacts with a flat plate placed parallel to the jet axis have been investigated experimentally. The flow is visualized using the schlieren technique, and the unsteady pressure on the flat plate as well as the sound pressure level in the far field are measured for different jet-plate separation distances. It is found that screech tone vanishes when the flat plate comes close to the jet axis. However, there is an azimuthal directivity in its propagation, which depends on jet-plate separation distance. In addition, the highly oscillating baseline jet flow is suppressed by the jet-plate interaction, and screech tone completely disappears when the jet-plate separation distance becomes less than 0.61 of the jet diameter.

Nomenclature

c	=	speed of sound
D	=	nozzle exit diameter
f_s	=	screech frequency
h	=	jet-plate separation distance, measured from the jet centerline to the plate surface
h_{critical}	=	critical jet-plate separation distance
L	=	shock-cell spacing
M	=	Mach number
M_c	=	large-scale disturbance convection Mach number
M_j	=	fully expanded Mach number
P_t	=	pressure inside the plenum chamber
p_∞	=	ambient pressure
r	=	radial distance from the nozzle exit
X, Y, Z	=	Cartesian coordinates
γ	=	specific heat ratio
θ	=	azimuthal angle of the microphone with respect to the flat plate
ψ	=	polar angle of the microphone with respect to the flat plate

I. Introduction

UNDER certain conditions, imperfectly expanded jets produce a discrete tone referred to as the screech. The screech is a loud discrete tone emitted by a supersonic jet when operated under offdesign conditions. The noise is produced by periodical coherent turbulent jet structures, which propagate upstream through a system of shocks and expansions formed by the jet flow and implant new disturbances into the shear layer near the nozzle lip. These disturbances travel downstream and grow, producing a jet instability mode. Repetition of this process results in a feedback loop, leading to the screech tone [1]. Understanding the screech and its effect on nearby structures is important, for example, for the design of advanced aircraft, because the screech can cause sonic fatigue failure [2]. In aeronautics and space sciences there are many applications that involve the impingement of an underexpanded jet on a solid boundary or object, such as multistage rocket separation, deep-space docking, space-module altitude-control thruster operation, lunar and planetary landing and takeoff, jet engine exhaust impingement of STOVL (short takeoff and vertical landing) aircraft, gas-turbine blade failure, and gun-muzzle blast impingement [3].

Lamont and Hunt [3] extensively studied the flowfield for single jet impingement on a flat plate at different angles, examining the mean pressure on the flat plate surface, as well as via shadowgraph visualizations. However, noise emission was not treated in their study. Ahuja et al. [4] and Kibens et al. [5] experimentally examined noise and instability waves in supersonic round jets in the proximity of a flat plate as well as a cylindrical wall. They clarified the effect of varying jet-plate separation distance on noise spectra using single-point sound-pressure-level (SPL) measurements. However, their results do not reveal enough of the screech-tone directivity characteristics. Seiner and Manning [6] studied the problem of jet-plate interaction for a rectangular jet, and Obase and Nakamura [7] investigated the same jet-plate interaction as reported in this study, using time-averaged measurements and single-point SPL measurements.

The recent research by Krothapalli et al. [8] deals with the flowfield and noise characteristics of supersonic jet impingement on a perpendicular flat plate in STOVL applications. They used more advanced measurement techniques such as particle image velocimetry. Lift loss due to the jet interaction is also reported in their study.

In the present study, experimental investigation of the interaction of an underexpanded supersonic jet with a flat plate, which was placed parallel to the jet axis, was carried out to obtain the screech-tone characteristics. In particular, the effect of jet-plate separation distance on screech-tone directivity in the far field is reported. In addition, pressure loads on the plate surface are examined by unsteady pressure measurements as well as visualizations of the flow structure near the plate surface. We can divide the whole flow region into two fields; one is the jet field on the jet side of the plate, and the

Received 10 February 2008; accepted for publication 5 March 2009.

*Assistant Professor, Aerospace Engineering Department, Graduate School of Engineering, Furo-cho, Chikusa-ku; khalil@nuae.nagoya-u.ac.jp. Senior Member AIAA.

†Graduate Student, Department of Aerospace Engineering; currently Engineer, Matsushita Eco-Systems, Ltd., Kasugai City, Aichi Prefecture 486-8522, Japan.

‡Graduate Student, Department of Aerospace Engineering; currently Engineer, Mitsubishi Heavy Industries, Ltd., Nagoya Aerospace Systems Works, 10 Oye-cho, Minato-ku, Nagoya 455-8515, Japan.

§Lecturer, Department of Aerospace Engineering, Graduate School of Engineering, Nagoya University, Furo-cho, Chikusa-ku; mori@nuae.nagoya-u.ac.jp. Member AIAA.

¶Professor, Department of Aerospace Engineering, Graduate School of Engineering, Nagoya University, Furo-cho, Chikusa-ku; nakamura@nuae.nagoya-u.ac.jp. Member AIAA.

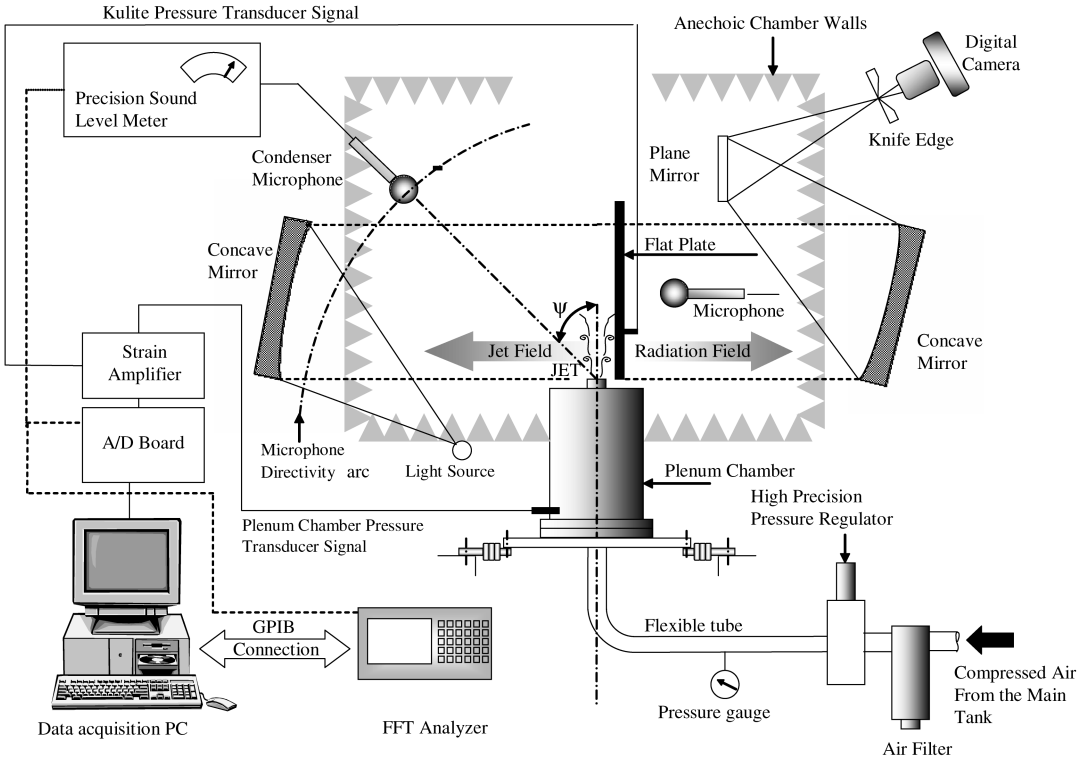

Fig. 1 Detailed schematic of the experimental facility at the Aerospace Engineering Department, Nagoya University.

other is the radiation field behind the plate, as shown in Fig. 1. Only sound emission in the jet field is studied in this paper.

II. Experimental Setup

Experiments were conducted in the open jet facility at the Department of Aerospace Engineering at Nagoya University. An underexpanded supersonic jet was exhausted inside an anechoic chamber, as shown in Fig. 1. The nozzle employed in the present study to produce the jet flow is a convergent (sonic) nozzle with an exit diameter of 10 mm, and its contour was designed as a simple fillet with a radius of 10 mm. The nozzle is attached to a cylindrical plenum chamber that has a diameter of 220 mm and a length of 400 mm. The plate, with which the jet interacts, is made of aluminum (5052) and has a length of 300 mm, a width of 200 mm, and a thickness of 10 mm. Figure 1 shows a detailed schematic of the jet facility.

High-pressure air is supplied from a tank with a volume of 12 m^3, and the air is stored at a pressure of 12 kgf/cm^2. This tank is connected to the plenum chamber via a high-pressure pipe with an inner diameter of 1 in. A high-precision pressure regulator and a solenoid valve are used to control the pressure inside the plenum chamber to within an accuracy of 0.25%. The solenoid valve is opened or closed via a signal that comes from the data acquisition PC (DAQ PC) with a data acquisition board (National Instruments, PCI-6035E) and a general-purpose interface bus (GPIB) board. The latter is used as an interface with a fast Fourier transform (FFT) analyzer; that is, by using the GPIB board, the data from the FFT analyzer are collected and the parameters are controlled.

The DAQ PC is connected to a 6-channel dc strain amplifier (KYOWA DPM-6H) with a frequency response of 5 kHz, which is in turn connected to various pressure transducers and load cells. Unsteady pressure measurements on the plate surface were made using an unsteady pressure transducer (Kulite XCS-062-15D). This transducer is connected to a single-channel dynamic dc strain amplifier (SAN-EI 6M71) with a frequency response of 100 kHz, the output of which is processed either by the FFT analyzer or the DAQ PC.

A microphone (RION UC-29 $\frac{1}{4}$ in. condenser microphone) is employed for SPL measurements and has a maximum resolution frequency of 100 kHz and a maximum SPL of 164 dB. This microphone can be traversed along an arc that is placed at a distance of 80D from the nozzle exit, where D is the diameter of the nozzle exit. The angle from the jet axis, ψ (referred to as the polar angle), can be varied from 15 to 110 deg, where 15 deg is in the downstream direction, and 110 deg is in the upstream direction. The azimuthal angle θ is the microphone location relative to the plate and can be varied from 0 deg to 90 deg, where 0 deg refers to the lateral direction along the plate surface, and 90 deg refers to the direction normal to the plate. The coordinate system employed in the present study is depicted in Fig. 2, along with the azimuthal and polar angles mentioned previously. This microphone is connected to the 2-channel multipurpose FFT analyzer (ONO-SOKKI CF-5210) to obtain SPL spectra. All of the SPL spectra reported in this study were acquired for frequencies up to 40 kHz with a constant bandwidth of 50 Hz, a sampling frequency of 102.4 kHz, and 10 averaged blocks with 800 data points in the spectra.

Each experiment was repeated 3 times. The pressure fluctuation values during the unsteady pressure measurements were found to be

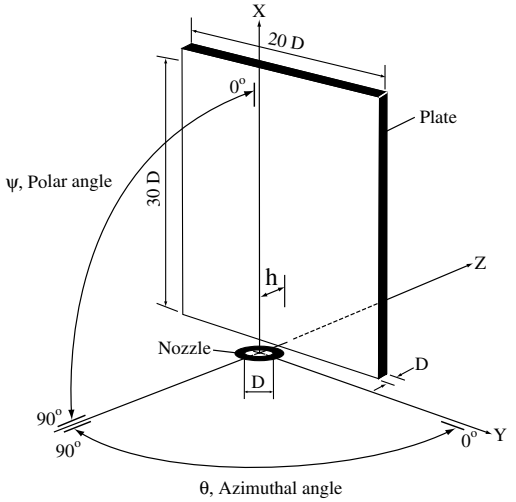

Fig. 2 Coordinate system.

highly repeatable, with a ±3% difference, which is not uncommon for such studies. For sound-pressure-level measurements, the issue of the fluctuation in plenum pressure, which changes the screech frequency and its amplitude, was carefully considered. The compressed air was supplied from a central facility which feeds many other test installations. Therefore, a certain amount of fluctuation was unavoidable. However, the plenum pressure, measured using a KYOWA PA-5KB pressure transducer, was continuously monitored and the data acquisition was performed only when the pressure remained within 0.25% of the desired setting. The accompanying drift in screech frequency was ±50 Hz and its amplitude was ±2 dB. This condition was imposed for all results presented in this paper. For the baseline jet, the reported SPL data were obtained at a single azimuthal angle, and it was assumed that those data are the same for other azimuthal angles, after it was confirmed that the maximum observed change in screech frequency was ±50 Hz and its amplitude was ±2 dB at other azimuthal angles.

The outside surfaces of the plenum chamber and other bodies placed in the near field were covered with two layers of an acoustically absorbent 6-mm-thick polyurethane foam to reduce the sound reflected from those objects. In data acquisition, transducer zero errors were monitored before each run, and the plenum (chamber) and ambient pressures were also checked for each run and were used to normalize the measured data.

The flow was also visualized using the conventional Töpler schlieren system with two 300-mm-diam and 2000-mm-focal-length parabolic mirrors and a pulsed Xenon light source of 10 μs duration. The knife edge was oriented vertically so that density gradients in the flow were along the axis of the plume. Density gradients are depicted by an increase in illumination in one direction and by a decrease in the opposite direction. A lens was used with a digital camera to provide a focused image of the plume. The plate surface flowfield was also visualized using the oil flow technique. For these oil flow experiments, the plate (painted black) was coated uniformly with a white mixture of titanium dioxide (for color) and liquid paraffin; oleic acid was added to the mixture to insure better dispersion of the titanium dioxide. The images produced via both the schlieren and oil flow techniques were obtained using a Canon EOS D30 digital camera with a resolution of 2160 × 1440 pixels.

III. Results and Discussion

The parameter M_j is used to represent the fully expanded Mach number of a sonic or supersonic jet. It is uniquely related to the pressure ratio P_t/p_∞, where P_t is the chamber pressure and p_∞ is the ambient pressure, and it is also referred to as the nozzle pressure ratio (NPR), through the following equation:

$$M_j = \left\{ \left[\left(\frac{P_t}{P_\infty} \right)^{\frac{\gamma-1}{\gamma}} - 1 \right] \frac{2}{\gamma - 1} \right\}^{1/2} \tag{1}$$

where γ is the specific heat ratio, and $\gamma = 1.4$ is used in the present study.

Most of the results presented here are for the case of $P_t/p_\infty = 5$, which corresponds to $M_j = 1.71$. This pressure ratio produces the screech-tone noise of a typical underexpanded circular jet issuing from a sonic nozzle.

The Mach number in the plume of an underexpanded sonic jet can actually exceed M_j. The pressure, as well as the Mach number, overshoots or undershoots this value in the fully expanded condition as flow passes through the shock-cell system. Note that M_j is nothing more than the exit Mach number of a fictitious nozzle, at the exit of which the flow expands up to the given NPR. In other words, it is an average jet Mach number in the region in which flow oscillates along the jet axis.

A. Visualization of the Jet-Plate Flowfield

Figure 3 shows both the instantaneous (spark) and time-averaged schlieren photographs for the baseline jet and for jet-plate interactions at different jet-plate separation distances; specifically,

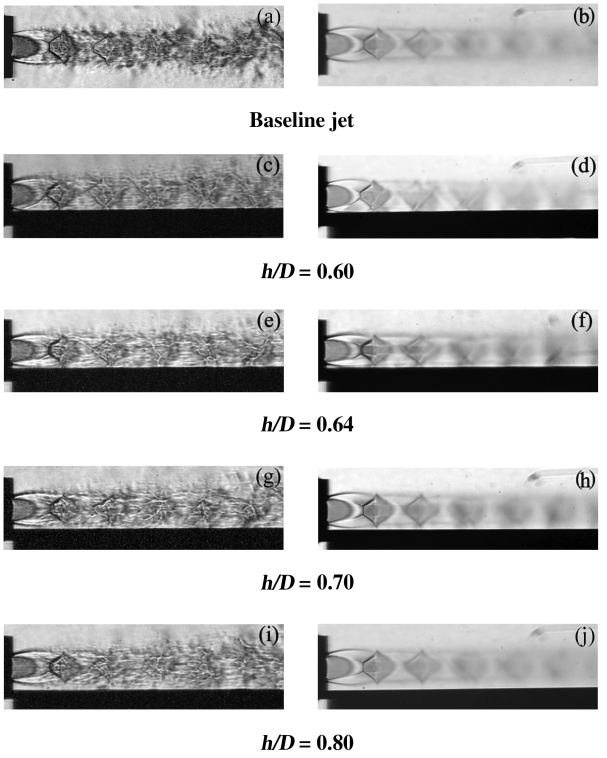

Fig. 3 Schlieren visualizations for different h/D; instantaneous (spark) photographs (left) and time-averaged photographs (right).

$h/D = 0.6$, 0.64, 0.7, and 0.8. Figures 3a and 3b show the baseline jet schlieren photographs for the instantaneous and time-averaged cases, respectively. The instantaneous photograph is characterized by the existence of a shock-cell structure and a large sinuous deformation of the jet. This is characteristic of a strongly screeching jet. The flow is sonic ($M = 1.0$) at the nozzle exit and expands in the downstream direction, because the jet static pressure at the exit is higher than the ambient pressure. The well-known shock-cell structure of the underexpanded sonic jet is clearly shown.

In the baseline jet, the jet leaves the nozzle with a laminar shear layer, and after a short distance, about one-third of the exit diameter, the layer breaks up and becomes turbulent. By comparing the time-averaged schlieren photograph and the instantaneous (spark) photograph, it is clear that the jet is highly unsteady in the downstream region after the first shock cell. In the time-averaged schlieren photograph, the shock cells following the initial one are blurred by large radial and axial oscillations of the jet as well as turbulent mixing. Sherman et al. [9] observed that an underexpanded sonic jet undergoes radial oscillations at the screech frequency, whereas the axial oscillations are not well correlated with the screech frequency.

Figures 3c and 3d show the instantaneous and time-averaged schlieren photographs, respectively, for a jet with the plate at $h/D = 0.6$. The interaction between the jet and plate is clearly seen; the attachment point of the jet to the plate is at about one-fourth of the exit diameter from the nozzle exit. It can also be observed that the first shock-cell length is slightly less than that for the baseline jet. This change in shock-cell length due to the plate may contribute to the change in screech frequency, compared with the baseline jet screech frequency, as will be discussed in Sec. III.C. A separation shock due to boundary-layer separation from the plate wall is observed at the end of the first shock cell, and this interacts with the barrel shock, resulting in two shock systems: a reflected shock and a bifurcation shock. This shock structure is repeated up until the fifth shock cell, as shown in the figure. Figure 4 shows the schlieren photograph and schematic of the shock structures at the third, fourth, and fifth shock cells for the case of $h/D = 0.6$.

An increase in h/D moves the jet attachment point downstream and promotes generation of the screech tone. Figures 3e and 3f show

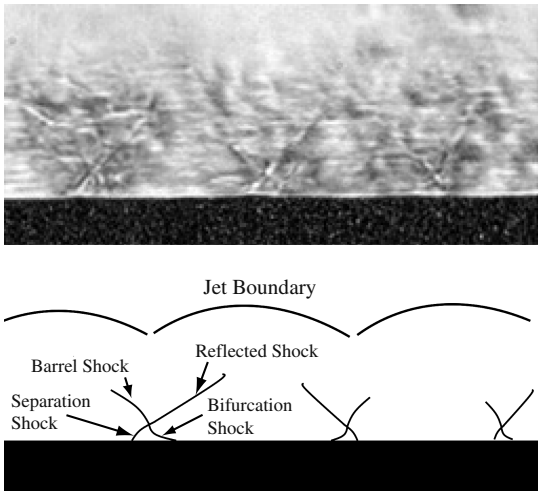

Fig. 4 Schlieren visualization and schematic of the third, fourth, and fifth shock cells for the case of $h/D = 0.60$.

the instantaneous and time-averaged schlieren photographs, respectively, for the case of $h/D = 0.64$. This case will be discussed in more detail later, because the highest unsteady pressure amplitude on the plate surface was observed at this jet-plate separation distance. The jet attachment point to the plate is clearly seen at about one-half of the exit diameter from the nozzle exit ($X/D = 0.5D$). The first shock-cell length increases compared with the case of $h/D = 0.6$ and becomes comparable with that of the baseline jet. The shock cells interact with the plate and produce different shock structures from those in the case of $h/D = 0.6$. Figure 5 shows the schlieren photograph and the schematic of the shock structures at the third, fourth, and fifth shock cells for the case of $h/D = 0.64$. The Y-shaped shock structure observed here consists of a separation shock, a barrel shock, and a reflected shock, and it is most pronounced at the third cell.

Further increase in h/D moves the attachment point toward further downstream, as shown in Figs. 3g–3j, which correspond to the cases of $h/D = 0.7$, 0.7, 0.8, and 0.8, respectively. The first shock-cell length is the same as that of the baseline jet. In these cases, generation of the screech tone is promoted, because the jet peripheral circumstances near the nozzle exit are not so largely disturbed as in the cases of $h/D = 0.6$ and 0.64. Thus, instability waves can survive rather longer, so that the discrete tones become noisier.

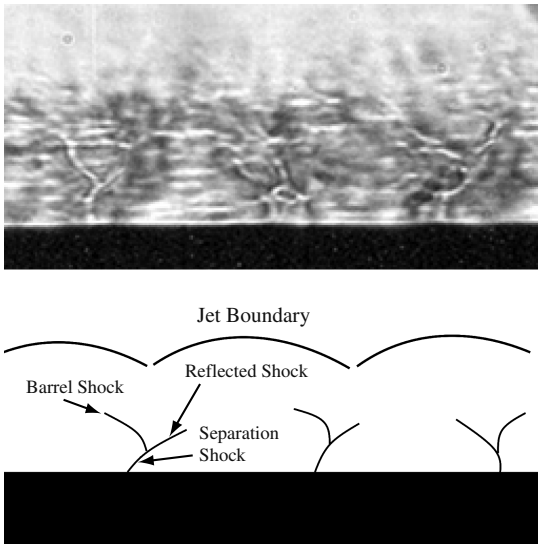

Fig. 5 Schlieren visualization and schematic of the third, fourth, and fifth shock cells for the case of $h/D \approx = 0.64$.

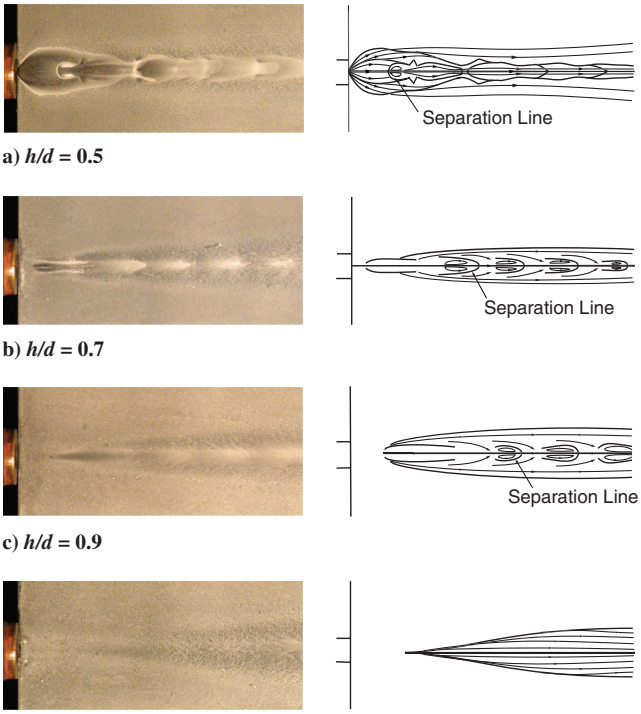

Fig. 6 Plate surface flow patterns visualized using oil flow at different plate jet-separation distances h/D.

Figures 6a–6d show plate surface flow patterns visualized using the oil flow technique at different jet-plate separation distances: specifically, $h/D = 0.5$, 0.7, 0.9, and 1.1. In the case of $h/D = 0.5$ (Fig. 6a), in which the jet is completely attached to the whole plate, the signature of the complex interaction flowfield on the plate surface is clearly captured by the oil flow. The first separation bubble near the nozzle exit is formed downstream of the separation shock. The separation shock interacts with the Mach disk, resulting in two shock systems: a reflected shock cell and bifurcation shock. Similar separation bubbles are also observed downstream. It is clearly confirmed from this oil flow that the first shock cell is strongly disturbed by the plate, and the screech tone has been suppressed.

Figure 6b shows the plate surface flow pattern for the case of $h/D = 0.7$. In this case, the jet attachment point to the plate moves slightly downstream. The first separation bubble is formed downstream of the separation shock and is observed in the schlieren photograph to occur at the end of the first shock cell. Similar separation bubbles are also observed in the downstream. In the case of $h/D = 0.9$ the separation bubbles are greatly weakened (Fig. 6c), and in the case of $h/D = 1.1$ they have disappeared (Fig. 6d).

From the schlieren photographs and the oil flow patterns on the plate surface, it is clear that an increase in the jet-plate separation distance h/D moves the attachment point of the jet further downstream, which has the potential to promote generation of the screech tone.

B. Unsteady Pressure Measurements on the Plate Surface

The spectra of the unsteady pressure fluctuations were acquired at different axial points on the plate surface along the x axis at $y/D = 0.0$ for different cases of jet-plate separation distance h/D; the measurement locations are $X/D = 5.2$, 6.9, 8.6, 10.2, and 11.8. The pressure level in each spectrum are decibels relative to 20 μ Pa.

The pressure spectra at $X/D = 5.2$ are shown in Fig. 7 for different jet-plate separation distances: $h/D = 0.5$, 0.6, 0.64, 0.7, and 0.8. For $h/D = 0.5$, the spectra are broadband without any discrete peaks, as shown in Fig. 7a. Increasing h/D, the spectral data show a high-amplitude discrete peak at a frequency of 8.6 kHz for $h/D = 0.64$, which is very close to the screech tone observed in this study. From

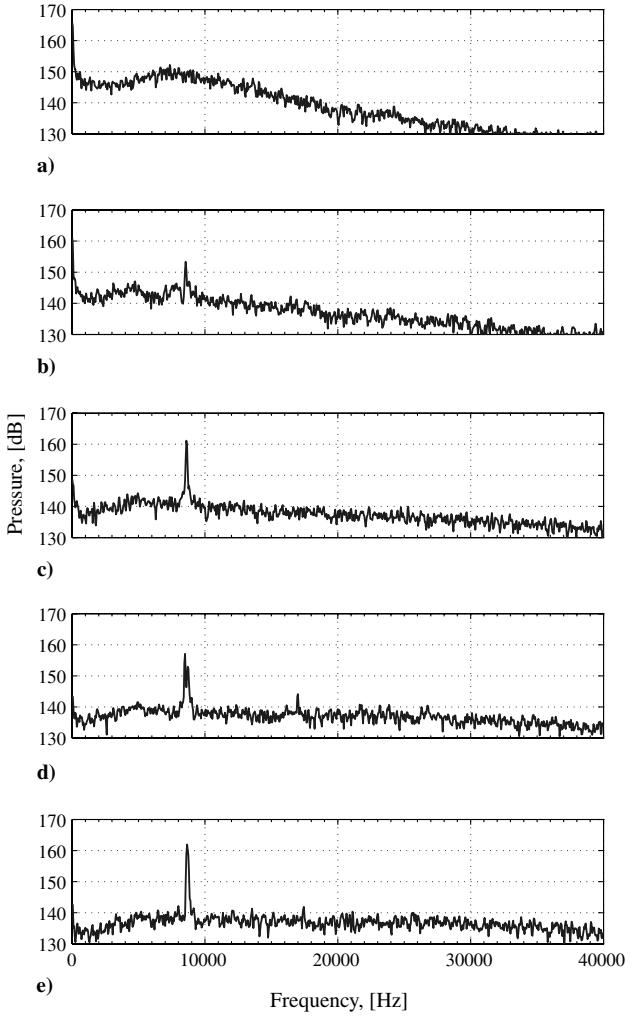

Fig. 7 Unsteady pressure spectra for $x/D = 5.2$: a) $h/D = 0.5$, b) $h/D = 0.6$, c) $h/D = 0.64$, d) $h/D = 0.7$, and e) $h/D = 0.8$.

Figs. 7b–7e, it is clearly seen that the amplitude of this peak increases up to $h/D = 0.64$ and then decreases, followed by another increase.

The amplitude of this discrete peak is plotted in Fig. 8 as a function of the jet-plate separation distance h/D, which is taken from the spectrum data in Fig. 7, along with the data for other axial locations. It is found from this result that the peak amplitude first increases until it reaches a local maximum at $h/D \simeq 0.64$ and then decreases until $h/D \simeq 0.7$. After that, it increases slowly. The distinct levels are observed almost at the same h/D, which is 0.64 for different X/D locations. The reason for this is that as jet-plate separation distance is

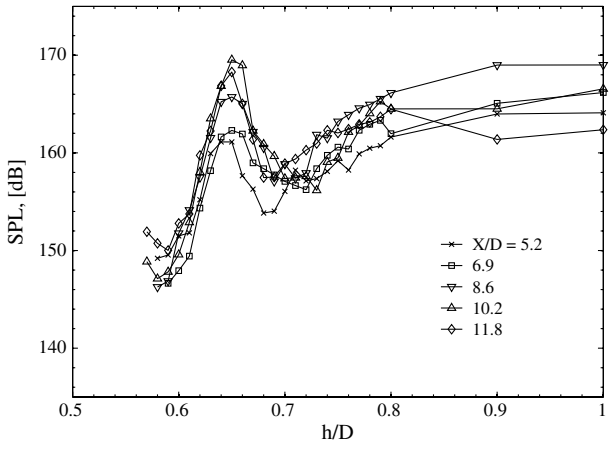

Fig. 8 Peak pressure fluctuation vs h/D at different axial locations.

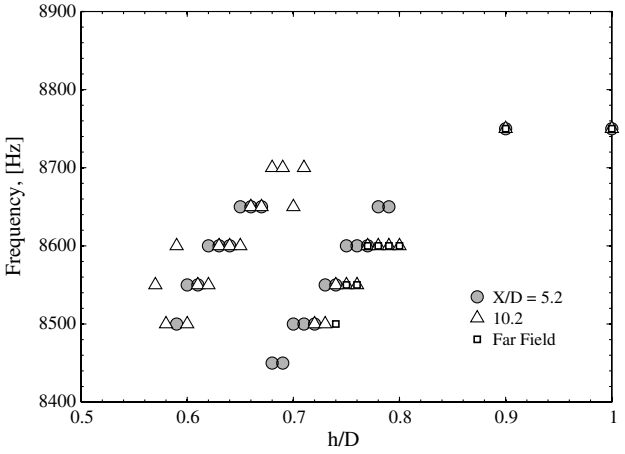

Fig. 9 Peak frequency vs h/D at different axial locations.

increased, the jet becomes locked onto the plate itself in the same manner as seen in the problem of twin plume coupling [10], in which instability waves of the plume have been locked onto those of an image plume that corresponds to the existence of a plate [4].

The frequency of these discrete peaks is plotted in Fig. 9 as a function of jet-plate separation h/D, taken from the spectral data in Fig. 7 for two different X/D locations: specifically, $X/D = 5.2$ and 10.2. The screech-tone frequencies acquired by a microphone are also presented in Fig. 9 and are denoted by "Far Field" when the

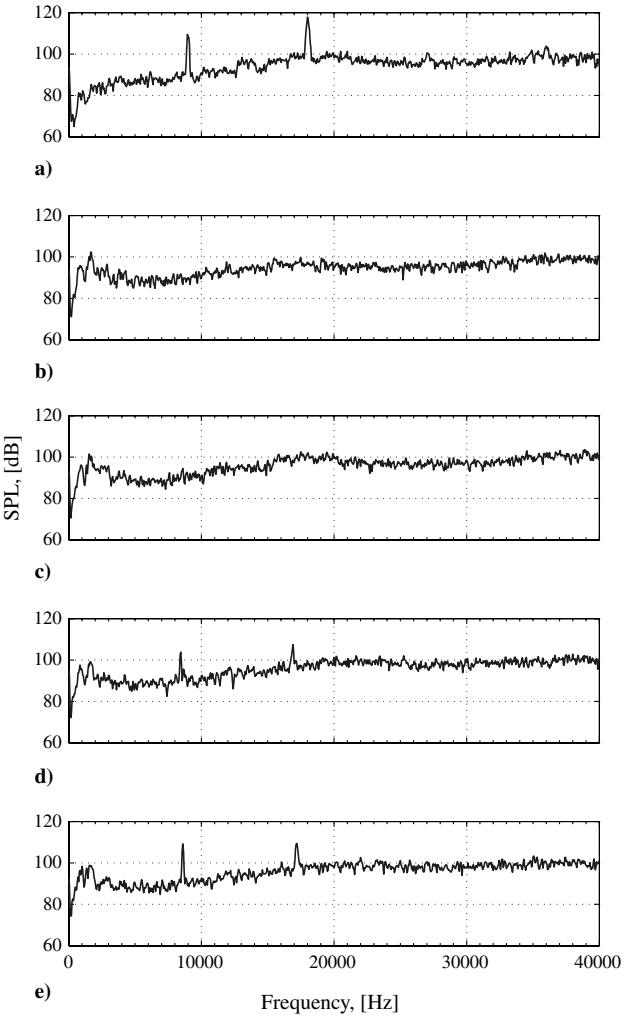

Fig. 10 SPL spectra for $\psi = 90\,\mathrm{deg}$ and $\theta = 90\,\mathrm{deg}$: a) baseline jet, b) $h/D = 0.6$, c) $h/D = 0.7$, d) $h/D = 0.8$, and e) $h/D = 0.9$.

microphone was located $80D$ away from the nozzle exit with $\theta = 90$ deg and $\psi = 90$ deg. Changes in the predominant frequency captured by the microphone in the far field are identical to those obtained using a pressure transducer at different plate surface locations. The change in screech frequency may be attributed to changes in the propagation speed of the instability waves or to changes in the shock-cell length, which will be discussed in the next section.

C. Sound-Pressure-Level Measurements

1. In the Normal Direction to the Plate ($\theta = 90$ deg)

The SPL spectra are shown in Fig. 10 as a function of jet-plate separation, in which $h/D = 0.6$, 0.7, 0.8, and 0.9, along with the baseline jet case. In this figure, a microphone is placed at a point located $80D$ away from the nozzle exit, with $\theta = 90$ deg and $\psi = 90$ deg. For the baseline jet, the first discrete tone is associated with the screech phenomenon of a shock-containing jet, the frequency of which is 8.95 kHz, and the second tone is the first harmonic, the frequency of which is 17.9 kHz. The screech tone does not manifest itself for the cases of $h/D = 0.6$ and 0.7, whereas for higher h/D values it is clearly observed. This confirms the dual-plume conclusion presented in Sec. III.B.

Note from this figure that the screech frequency shifts from that of the baseline jet by a few hundred hertz as h/D is decreased; specifically, the screech frequency is about 8.95 kHz for the baseline jet, whereas it is reduced to 8.75 kHz for $h/D = 0.9$. One possible cause for this change is a change in the attachment point of the jet to the plate, which could change the shock-cell spacing. The other possible cause is a change in the propagation speed of the instability waves. At small jet-plate separation distances, the convection Mach number of the instability waves may be decreased by viscous interactions [4]. The screech frequency f_s can be predicted from the following expression [6]:

$$f_s = \frac{cM_c}{L(1 + M_c)} \tag{2}$$

where c is the speed of sound, M_c is the large-scale disturbance convection Mach number, and L is the plume/shock-cell spacing.

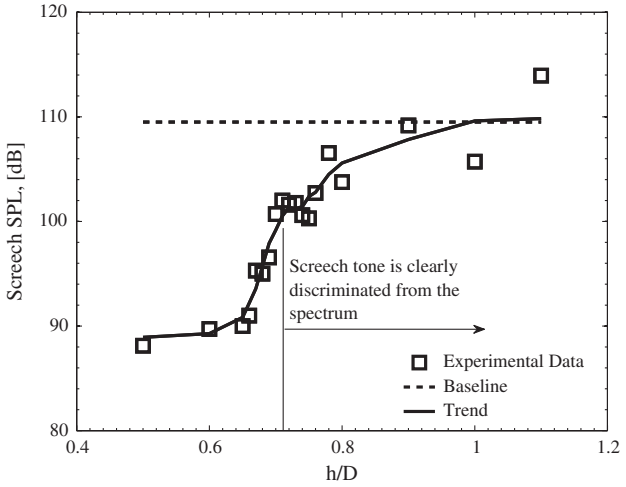

Fig. 11 Effect of jet-plate separation h/D, on the SPL which corresponds to screech tone. Microphone is placed at $r = 80D$, $\psi = 90$ deg, and $\theta = 90$ deg.

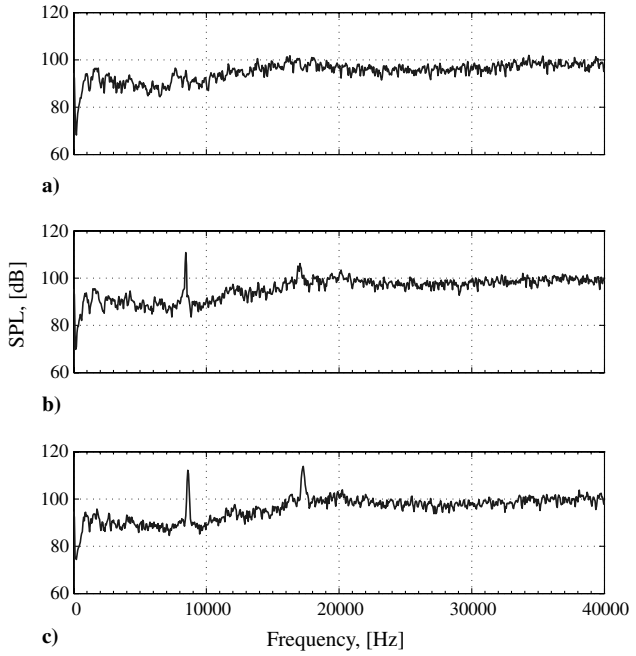

Fig. 12 SPL spectra for $\theta = 45$ deg and $\psi = 90$ deg: a) $h/D = 0.6$, b) $h/D = 0.7$, and c) $h/D = 0.8$.

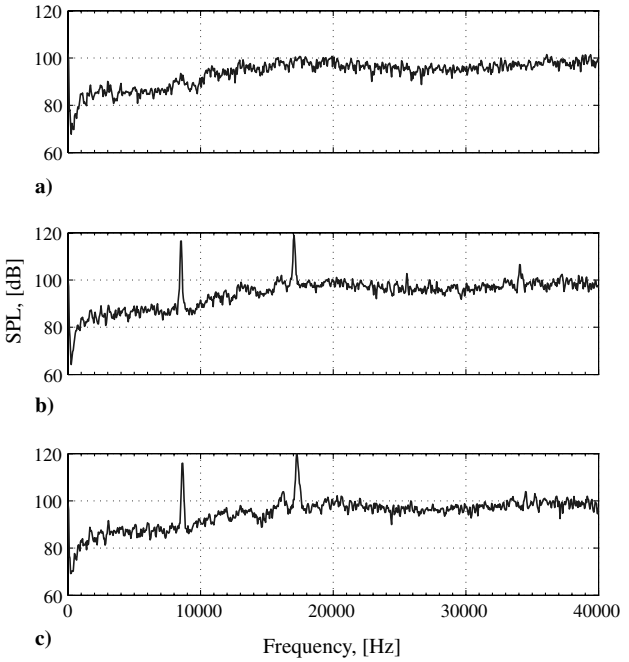

Fig. 13 SPL spectra for $\theta = 0$ deg and $\psi = 90$ deg: a) $h/D = 0.6$, b) $h/D = 0.7$, and e) $h/D = 0.8$.

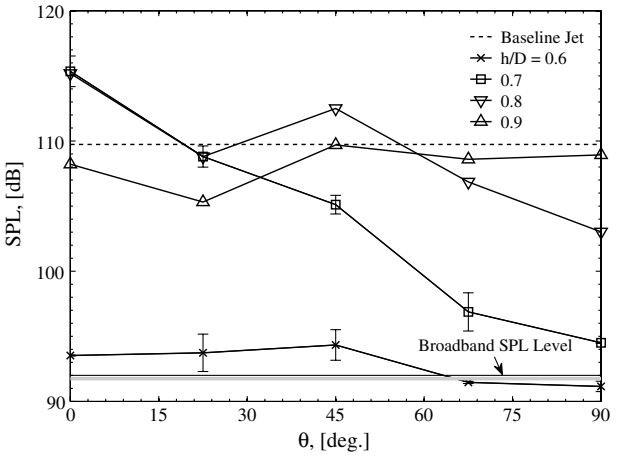

Fig. 14 Screech SPL vs azimuthal angle with h/D as parameter for $\psi = 90$ deg.

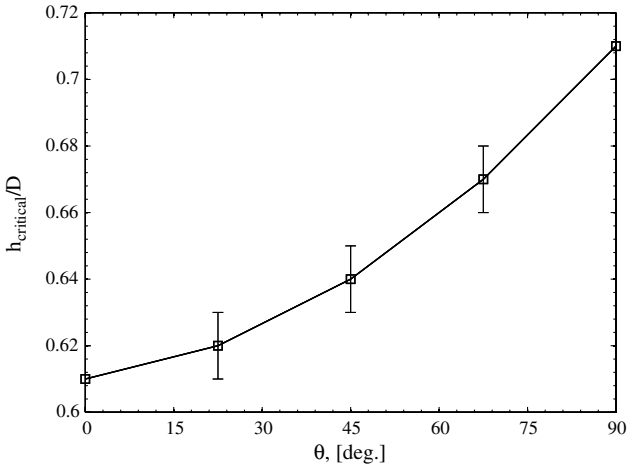

Fig. 15 Minimum h/D value for detectable screech tone in SPL spectra at different azimuthal angles for $\psi = 90$ deg.

From the schlieren photographs shown in Fig. 3j, L could be assumed constant. Therefore, it is clear from Eq. (2) that decreasing M_c will reduce the screech frequency.

Variations in the screech amplitude (SPL) are plotted in Fig. 11 as a function of jet-plate separation h/D, taken from the spectral data in Fig. 10. The trend line presented in this figure was plotted by averaging the scattered data points using the five neighboring data points at each valve of h/D. Basically, with decreasing h/D, low-frequency noise is increased due to jet-plate interaction. Bringing the plate close to the jet (i.e., decreasing the value of h/D from 1.1 to 0.8), first the SPLs that correspond to the screech tone are slowly reduced, and then from around $h/D = 0.8$ they rapidly fall.

2. *At Different Azimuthal Angles*

SPL spectra at another two azimuthal locations, $\theta = 45$ and 0 deg, are shown in Figs. 12 and 13, respectively, in which ψ is held constant at 90 deg, and the distance between the microphone and the nozzle exit is the same as before (i.e., $r = 80D$). The results are presented for $h/D = 0.6$, 0.7, and 0.8 in both figures. It is noted that as θ decreases, the SPL of the screech tone increases for the cases $h/D = 0.7$ and 0.8. In the same way as seen in Fig. 10, for $h/D = 0.6$ the screech tone does not manifest itself at these two azimuthal locations. Again this confirms the dual-plume conclusion presented in Sec. III.B.

The screech amplitude (SPL) is plotted in Fig. 14 as a function of azimuthal angle θ and jet-plate separation h/D, based on the spectral data in Figs. 10, 12, and 13. The baseline jet screech-tone amplitude is 109.5 dB, shown as a horizontal dotted line in Fig. 14. Similarly, the average value of the broadband SPL in the vicinity of the screech tone, which is 92 dB, is depicted by a solid gray line in Fig. 14. This value is regarded as a limiting value to discriminate the screech tone from the spectra. In the case of $h/D = 0.6$, the screech tone is only

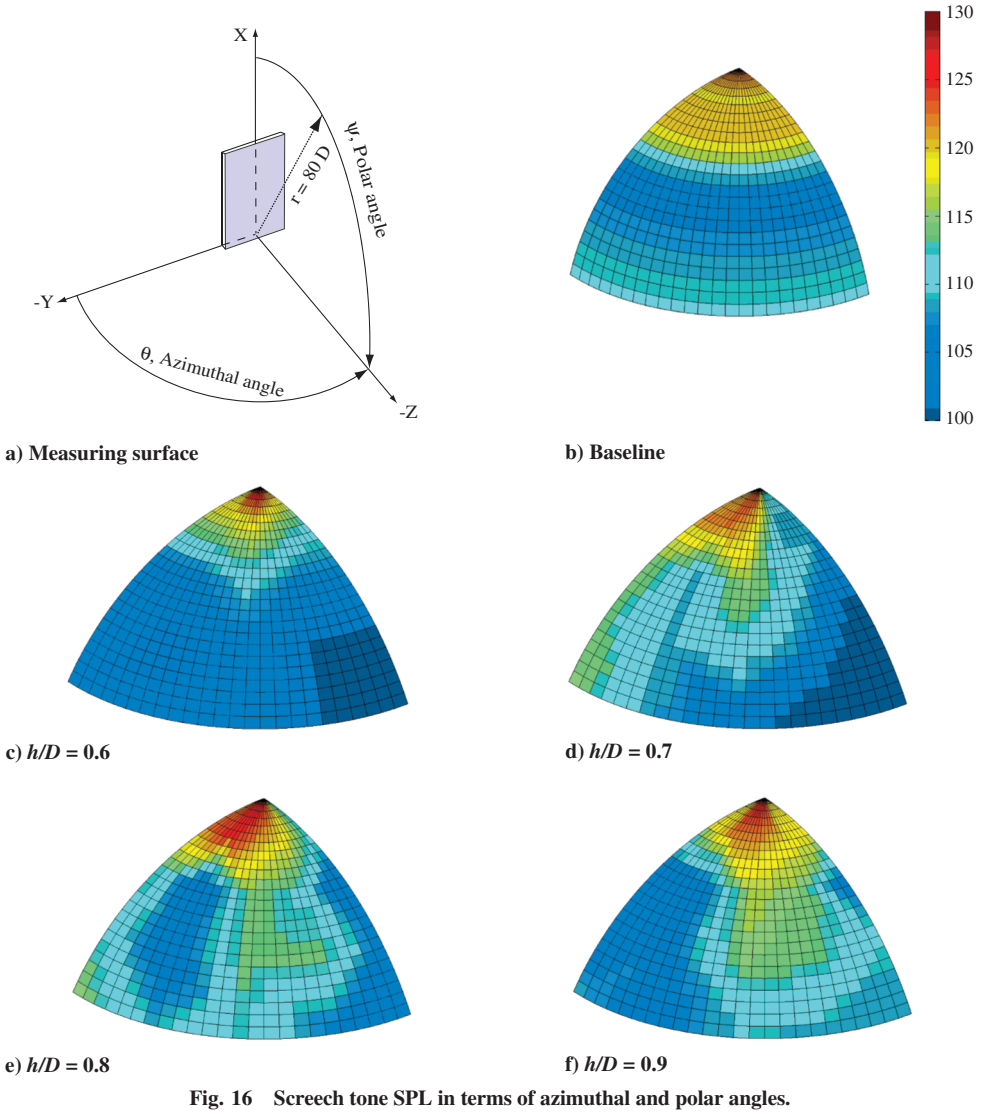

a) Measuring surface

b) Baseline

c) h/D = 0.6

d) h/D = 0.7

e) h/D = 0.8

f) h/D = 0.9

Fig. 16 Screech tone SPL in terms of azimuthal and polar angles.

slightly displaced from the average broadband SPL limiting line, although a slight increase in SPL is observed for $\theta \leq 45$ deg.

For $h/D = 0.7$ the screech SPL is well above the limiting average broadband SPL level, and the screech-tone SPL decreases with increasing azimuthal angle. A similar tendency can be seen for $h/D = 0.8$. The case for $h/D = 0.9$ shows an almost constant SPL with azimuthal angle, the magnitude being comparable with that of the baseline jet. This high screech-tone directivity for certain values of jet-plate separation distance is an important finding in the present investigation.

As mentioned previously, screech tone is not clearly detected for the case of $h/D = 0.6$. To obtain the critical value of the jet-separation distance for a given azimuthal angle, beyond which screech tone manifests itself in the SPL spectra, the jet-plate separation distance was varied at smaller intervals, starting from $h/D = 0.6$ with a step size $\Delta h/D$ of 0.01. Thus, the separation distance at which the screech tone becomes detectable in the SPL spectra was recorded and is designated as h_{critical}/D. This procedure was repeated for different azimuthal angles. Figure 15 shows variations in h_{critical}/D in terms of the azimuthal angle θ. The vlaue of h_{critical}/D increases with θ, where $h_{\text{critical}}/D = 0.61$ at $\theta = 0$, and $h_{\text{critical}}/D = 0.71$ at $\theta = 90$ deg. Actually, at $h/D = 0.61$ the screech tone was observed in the SPL spectra at $\theta = 0$ deg. Based on the aforementioned observation, it can be stated that the screech tone starts to be detectable from the SPL spectrum of a jet-plate separation distance of 0.61. Even for $h/D > 0.71$, the directivity of the screech tone is strongly dependent on h/D, although it becomes attenuated for high h/D values.

This directional behavior of the emitted pressure waves was also observed by Seiner et al. [10] for twin supersonic plume resonance. In their study, they observed that the minimum pressure amplitude was observed for pressure waves radiated at angles normal to the flapping plane of the twin jet. The jet in the present study becomes locked onto the plate in the same manner as seen in the problem of twin plume coupling, in which instability waves of the plume have been locked onto those of an image plume due to the existence of a plate. The minimum pressure amplitude was observed at $\theta = 90$ deg, as shown in Fig. 14.

This finding is summarized in Fig. 16, in which the directivity patterns for the screech tone are presented as three-dimensional views for different separation distances. Specifically, screech SPLs are plotted at various values of azimuthal angle θ and polar angle ψ for $h/D = 0.6$, 0.7, 0.8, and 0.9 as well as for the baseline jet. The dependence of screech-tone directivity on h/D is clearly appreciated from this figure.

IV. Conclusions

The screech-tone characteristics of a round underexpanded sonic jet in the vicinity of a flat plate for different jet-plate separation distances have been investigated experimentally. Based upon the results presented previously, the following conclusions can be drawn.

1) An increase in the jet-plate separation distance reduces the viscous interaction with the plate and hence increases the disturbance convection Mach number, which in turn increases the screech frequency and promotes the generation of a screech tone.

2) At a jet-plate separation distance h/D of 0.64, the jet becomes locked onto the plate in a similar manner as observed for the phenomenon of twin plume coupling (i.e., instability waves of the jet plume become locked on to those of its image plume).

3) The predominant frequency of flow fluctuations on the plate surface measured by a pressure transducer is identical with the acoustic frequency measured by a microphone in the far field; the value itself changes slightly with jet-plate separation distance.

4) The directional behavior of the emitted pressure waves confirms that the present jet becomes locked onto the plate in the same manner as seen in the problem of twin plume coupling. The minimum pressure amplitude was observed at $\theta = 90$ deg.

Acknowledgments

This work was performed while Mohammed K. Ibrahim was on sabbatical from the Faculty of Engineering, Aerospace Engineering Department, University of Cairo, Egypt. The first author is grateful to Atsushi Hashimoto, Michael Jones, and Igor Men'shov for their valuable discussions and fruitful advice. The authors would like to thank the reviewers for their comments that help improve the manuscript.

References

[1] Powell, A., "The Noise of Choked Jets," *Journal of the Acoustical Society of America*, Vol. 25, No. 3, May 1953, pp. 385–389. doi:10.1121/1.1907052

[2] Raman, G., "Supersonic Jet Screech: Half-Century from Powell to the Present," *Journal of Sound and Vibration*, Vol. 225, No. 3, 1999, pp. 543–571. doi:10.1006/jsvi.1999.2181

[3] Lamont, P. J., and Hunt, B. L., "The Impingement of Underexpanded Axisymmetric Jets on Perpendicular and Inclined Flat Plates," *Journal of Fluid Mechanics*, Vol. 100, No. 3, 1980, pp. 471–512. doi:10.1017/S0022112080001255

[4] Ahuja, K. K., McCaulley, J. A., and Tam, C. K. W., "Noise and Instability Waves in Supersonic Jets in the Proximity of Flat and Cylindrical Walls," AIAA 12th Aeroacoustics Conference, AIAA Paper 89-1136, San Antonio, TX, Apr. 1989.

[5] Kibens, V., Saripalli, K. R., Wlezien, R. W., and Kegelman, J. T., "Unsteady Features of Jets in Lift and Cruise Modes for VTOL Aircraft," *Proceedings of the International Powered Lift Conference*, P-203, Society of Automotive Engineers, Warrendale, PA, 7–10 Dec. 1987, pp. 543–552; also Society of Automotive Engineers Paper 872359.

[6] Seiner, J. M., and Manning, J. C., "Supersonic Jet Plume Interaction with a Flat Plate," *Proceedings of the International Powered Lift Conference*, P-203, Society of Automotive Engineers, Warrendale, PA, 7–10 Dec. 1987, pp. 563–573; also Society of Automotive Engineers Paper 872361.

[7] Obase, K., and Nakamura, Y., "Aerodynamic and Aeroacoustic Interaction of a High-Speed Jet with a Flat Plate," 2nd AIAA Flow Control Conference, AIAA Paper 2004-2404, Portland, OR, 2004.

[8] Krothapalli, A., Rajkuperan, E., Alvi, F., and Lourenco, L., "Flow Field and Noise Characteristics of a Supersonic Impinging Jet," *Journal of Fluid Mechanics*, Vol. 392, 1999, pp. 155–181. doi:10.1017/S0022112099005406

[9] Sherman, P. M., Glass, D. R., and Duleep, K. G., "Jet Flow Field During Screech," *Applied Scientific Research*, Vol. 32, 1976, pp. 283–303. doi:10.1007/BF00411780

[10] Seiner, J. M., Manning, J. C., and Ponton, M. K., "Dynamic Pressure Loads Associated with Twin Supersonic Plume Resonance," *AIAA Journal*, Vol. 26, No. 8, Aug. 1988, pp. 954–960. doi:10.2514/3.9996

E. Gutmark
Associate Editor